# Kinetic electron emission induced by grazing scattering of heavy ions from metal surfaces

Yuan-Hong Song* and You-Nian Wang
*The State Key Laboratory of Materials Modification by Laser, Electron, and Ion Beams, Department of Physics, Dalian University of Technology, Dalian 116023, People's Republic of China*

Z. L. Mišković
*Department of Applied Mathematics, University of Waterloo, Waterloo, Ontario, Canada N2L 3G1*
(Received 19 February 2003; published 27 August 2003)

The angle-resolved energy spectra of the electrons emitted from a metal surface during specular reflection of heavy ions have been studied by means of the first-order, time-dependent perturbation theory, with the electron states obtained from a finite step-barrier potential model. The surface response has been described by the dielectric formalism within the specular reflection model, where the local-field correction and the plasmon-pole approximation have been used for the dielectric function in the cases of low and high ion velocities, respectively. The ion trajectory has been evaluated based on the surface continuum potential and the ion image potential, whereas the screening of the ion by the bound electrons has been taken into account by means of the Brandt-Kitagawa model. It has been found that the electron spectra are dominated by the decay of surface plasmons for fast incident ions, whereas the electron emission is dominated by the single-electron excitation mechanism for slow incident ions.

DOI: 10.1103/PhysRevA.68.022903 PACS number(s): 34.50.Bw, 34.50.Dy

## I. INTRODUCTION

The interactions of accelerated ions with solid surfaces, including the inelastic energy-loss processes, the charge exchange, and the secondary emission phenomena, have been the subject of many experimental and theoretical studies [1–4]. Special attention has been paid to the ion-surface grazing scattering owing to its prolonged interaction times with the surface and the extreme sensitivity to the surface properties. When an energetic ion approaches a solid surface, it loses its kinetic energy due to ionization and excitation of the electrons in the solid via dynamically screened Coulomb interactions. While the excitation of the electrons bound to the surface atoms is only important under the large-angle scattering conditions, the energy losses during the glancing-angle incidence on the surface are dominated by the excitations of the valence-band electrons in the near-surface region. Thus, in the case of grazing scattering, the excitation processes in the valence band include two mechanisms: the collective excitations giving rise to the surface-plasmon field, and the single-particle excitations of the quasi-free-electrons via binary collisions with the projectile.

The so-called kinetic electron emission (KEE) is generally perceived as being closely related to the projectile energy losses, where the excited target electrons are transported and emitted through the surface into vacuum. When the projectile approaches the surface under planar channeling conditions, the electron emission originates from the region just above the topmost atomic layer of the solid, so that the multiple inelastic scattering during the transport of electrons towards the surface plays minor role in the spectra of emitted electrons. Then, the energy spectra of emitted electrons are determined by the characteristics of the excitation mechanism and by the transmission across the surface. While the spectra of KEE due to single-electron excitation are generally smooth, the plasmon excitation mechanism can give rise to electron emission, owing to the decay of plasmon into the electron-hole pairs, which can be emitted with a characteristic peak structure.

The excitation of plasmons in the bulk and at the surface of solid targets by fast charges has been studied for some time. Most of the experimental studies have used fast projectiles which can excite plasmons via direct Coulomb interaction [5–7]. However, an increasing attention has been focused in the past several years on the plasmon excitation induced by slow ions. Although this mechanism is not expected to operate under such conditions due to the conservation of energy and momentum restrictions, several recent experimental studies [8–15] have reported characteristic features in the emitted electron energy spectra induced by slow ions, which can be ascribed to the plasmon excitation and decay mechanism. Several explanations of this effect have been discussed, but detailed interaction mechanism for plasmon excitation by slow ions is still not understood completely.

From the theoretical point of view [16], the energy spectra of the electrons emitted from the surface can be deduced from calculations of the energy-loss rate experienced by a charged particle due to the creation of the electron-hole pairs. Furthermore, the first-order perturbation theory has been used to describe the ion-induced electron emission [17,18] for ions traveling on trajectories which are parallel or normal to the surface, where the surface wake potential was described by means of the specular-reflection model (SRM) [19,20], and the electron wave functions were used, which take the presence of the surface into account. These studies showed that the energy distributions of the emitted electrons contain features which originate in the deexcitation of plasmons. On the other hand, the role of single-electron excita-

*Email address: songyh@dlut.edu.cn

 

tions in the electron emission, produced by the screened Coulomb interaction between the incident ion and the surface electrons, has been studied by means of the first Born approximation [21,22]. It has been found that this mechanism provides the dominant contribution, in comparison with the experimental data, to the electron emission for angles far from the direction of specular reflection of the projectile. In addition, while neglecting the plasmon decay mechanism, the SRM model has been modified [23,24] and used to study the binary collisions with the free-electron gas, giving the results which compared well with the experimental data for large ejection angles of electrons. Finally, as an alternative to the plasmon excitation and decay mechanism, the interference arising from the decay of surface Bloch waves via scattering on surface atoms has been recently proposed [25] as responsible for the characteristic features in the electron emission spectra induced by grazing scattering of slow ions.

In this work, we attempt to describe the contributions to the KEE spectra from both the collective and the single-electron excitations under the grazing scattering conditions by using the dielectric function theory. In our previous work [26], we had developed a theoretical model to simulate the position-dependent stopping power, the scattering trajectory, and the energy loss for heavy ions, grazingly scattered from a solid surface. The fact that such a model gave reasonably good comparison with the experimental data [27,28] lends some confidence in the present calculations of the differential electron emission probabilities. These probabilities are obtained by means of the first-order perturbation theory [17,18], where the ion-electron interaction is described by the surface wake potential deduced from the SRM model, with different expressions when the ions move above, or in the interior of, the solid surface. In particular, the dielectric model is used with the local-field correction when considering slow ions, whereas the plasmon-pole approximation is used for fast ions. Since we are concerned with the electron emission induced by heavy ions, the distribution of electrons bound to the projectile and the concomitant effective charge state of the projectile are taken into account. The work is organized as follows. In Sec. II, we describe the theoretical model of the electron emission. The analysis of the grazing scattering trajectory for heavy ions is presented in Sec. III. The results of our calculation are presented in Sec. IV, while Sec. V contains our concluding remarks. Atomic units, where $m_e=\hbar=e=1$, are used unless otherwise stated.

## II. MODEL FOR ELECTRON EMISSION

We consider a heavy projectile incident on a solid surface under a glancing angle $\alpha$ and place a coordinate system in the scattering plane, with the $x$ axis parallel to the surface and the $z$ axis perpendicular to it. The coordinate center ($x=0$, $z=0$) is placed at the electron gas edge of the solid surface, such that the region $z<0$ is occupied by the electron gas of the bulk of the solid. The notations $\mathbf{r}=(\mathbf{R},z)$, $\mathbf{k}=(\mathbf{Q},k_z)$, and $\mathbf{v}=(\mathbf{v}_\parallel,v_z)$ will be used, where $\mathbf{R}$, $\mathbf{Q}$, and $\mathbf{v}_\parallel$ represent the components parallel to the surface.

We consider here only the situation where the projectiles are reflected from the first atomic layer, so that the angles of the incidence $\alpha$ should be of the order of milliradians, characterizing planar channeling. The ion distance $z_0$ evolves adiabatically, that is, on a time scale much longer than the other characteristic time scales of the problem. The total charge density of the projectile is

$$\rho_{ext}(\mathbf{r},t)=[Z_1\delta(\mathbf{R}-v_\parallel t)-\sigma_n(\mathbf{R}-\mathbf{v}_\parallel t)]\delta(z-z_0), \quad (1)$$

where $Z_1$ is the atomic number of the projectile and $(\mathbf{v}_\parallel t,z_0)$ is its position vector, while $\sigma_n(\mathbf{R})=\int\rho_n(\mathbf{r})\,dz$ is the two-dimensional projection of the full three-dimensional distribution $\rho_n(\mathbf{r})$ of the electrons bound at the projectile. Using the statistical model of Brandt and Kitagawa (BK) [29] for $\rho_n(\mathbf{r})$ enables one to express the Fourier transform of the total charge density as follows:

$$\tilde{\rho}_{ext}(\mathbf{k},\omega)=2\pi\tilde{\sigma}_n(Q)\,\delta(\omega-\mathbf{Q}\cdot\mathbf{v}_\parallel)e^{ik_zz_0}, \quad (2)$$

where $\tilde{\sigma}_n(Q)=Z_1[q(z_0)+(Q\Lambda)^2]/[1+(Q\Lambda)^2]$, with $\Lambda$ being the screening length [29], $q(z_0)=1-N_n(z_0)/Z_1$ the ionization degree, and $N_n(z_0)$ the number of electrons bound at the ion located at $z_0$.

The surface response to the incident ions is obtained by means of the SRM model, in which the dispersion effects are incorporated by expressing the surface response in terms of the bulk dielectric function. In this model, the electrons which constitute the response of the medium are considered to be specularly reflected at the surface, whereas the electronic charge density vanishes outside the surface. Thus, assuming that the ion moves on a trajectory parallel to the surface, the induced potential is given by [30]

$$\begin{aligned}\phi(\mathbf{Q},\omega,z)=&\frac{(2\pi)^2\tilde{\sigma}_n(Q)\,\delta(\omega-\mathbf{Q}\cdot\mathbf{v}_\parallel)}{Q}\\&\times\left\{\left[\frac{2e^{-Qz_0}}{1+\epsilon_s(Q,\omega)}\epsilon_s(Q,\omega,z)\right]\theta(-z)\right.\\&\left.+\left[\frac{\epsilon_s(Q,\omega)-1}{\epsilon_s(Q,\omega)+1}e^{-Q(z+z_0)}+e^{-Q|z-z_0|}\right]\theta(z)\right\}\end{aligned} \quad (3)$$

when the ion is in the vacuum and by

$$\begin{aligned}\phi(\mathbf{Q},\omega,z)=&\frac{(2\pi)^2\tilde{\sigma}_n(Q)\,\delta(\omega-\mathbf{Q}\cdot\mathbf{v}_\parallel)}{Q}\left\{\left[\epsilon_s(Q,\omega,z_0-z)\right.\right.\\&+\epsilon_s(Q,\omega,z_0+z)\\&\left.-\frac{2\epsilon_s(Q,\omega,z)\epsilon_s(Q,\omega,z_0)}{1+\epsilon_s(Q,\omega)}\epsilon_s(Q,\omega,z)\right]\theta(-z)\\&\left.+\left[\frac{2\epsilon_s(Q,\omega,z_0)}{\epsilon_s(Q,\omega)+1}e^{-Qz}\right]\theta(z)\right\}\end{aligned} \quad (4)$$

when the ion moves in the interior of the solid. Here, $\theta$ is the unit step function, $\epsilon_s(Q,\omega,z)$ is the surface dielectric function which can be expressed in terms of the bulk dielectric function $\epsilon(k,\omega)$ as follows:

$$\epsilon_s(Q,\omega,z)=\frac{Q}{\pi}\int \frac{dk_z}{k^2}\frac{e^{ik_z z}}{\epsilon(k,\omega)}, \tag{5}$$

and $\epsilon_s(Q,\omega)=\epsilon_s(Q,\omega,z=0)$.

Describing the solid in the jellium approximation, the electrons are considered to be free within the solid, and confined in the $z<0$ region by a step potential $V=V_0\theta(z)$, where $V_0=E_F+\Phi$, with $E_F$ being the Fermi energy and $\Phi$ the work function. Using the first-order, time-dependent perturbation theory, the solutions of the Schrödinger equation for the electron states with the step potential barrier are [17]

$$\psi_l^\sigma(r)=\frac{e^{i\mathbf{l}_\parallel\cdot\mathbf{R}}}{\sqrt{2\pi A}}\varphi_{l_z}^\sigma(z), \tag{6}$$

where $A$ is the area of the surface, $\mathbf{l}=(\mathbf{l}_\parallel,l_z)$ is the momentum of the electron on the solid side, while $\sigma$ stands for the character of the state, including the bound states, $\sigma=0$ (with $l_z^2\leqslant 2V_0$),

$$\varphi_{l_z}^0(z)=\left(\frac{l_z-ip}{l_z+ip}e^{-il_z z}+e^{il_z z}\right)\theta(-z)+\frac{2l_z}{l_z+ip}e^{-pz}\theta(z), \tag{7}$$

outgoing states, $\sigma=+$,

$$\varphi_{l_z}^+(z)=\left(\frac{l_z-\kappa_z}{l_z+\kappa_z}e^{-il_z z}+e^{il_z z}\right)\theta(-z)+\frac{2l_z}{l_z+\kappa_z}e^{i\kappa_z z}\theta(z), \tag{8}$$

and incoming states, $\sigma=-$,

$$\varphi_{l_z}^-(z)=\sqrt{\frac{l_z}{\kappa_z}}\left[\frac{2\kappa_z}{\kappa_z+l_z}e^{-il_z z}\theta(-z)+\left(\frac{\kappa_z-l_z}{\kappa_z+l_z}e^{i\kappa_z z}+e^{-i\kappa_z z}\right)\theta(z)\right], \tag{9}$$

where $p=\sqrt{2V_0-(l_z^0)^2}$, while $\kappa_z=\sqrt{(l_z)^2-2V_0}$ is the normal component of the electron momentum in vacuum. Let us denote the initial and the final momenta of the electron by $\mathbf{l}_0=(\mathbf{l}_\parallel^0,l_z^0)$ and $\mathbf{l}_1=(\mathbf{l}_\parallel^1,l_z)$, so that the initial and the final energies of the electron are $\varepsilon_0=l_0^2/2$ and $\varepsilon_1=l_1^2/2$, respectively. Using the asymptotic wave functions for the final states of the excited electrons, which have been applied to the case of surface electron emission, Bethe [31] and Wilems [32] have obtained the approximate expression for the perturbed wave function in terms of the screened potential,

$$\triangle\psi(\mathbf{r},t)=\frac{1}{\sqrt{2\pi A}}\int d\boldsymbol{\kappa}e^{-i\boldsymbol{\kappa}\cdot\mathbf{r}}e^{-i\varepsilon_1 t}\theta(\kappa_z(t-t_0)-z)\mathbf{M}_{\boldsymbol{\kappa}\leftarrow\mathbf{l}_0}. \tag{10}$$

Here, $\mathbf{M}_{\boldsymbol{\kappa}\leftarrow\mathbf{l}_0}$ represents the transition amplitude,

$$\mathbf{M}_{\boldsymbol{\kappa}\leftarrow\mathbf{l}_0}=\frac{-i}{(2\pi)^2}\left(\frac{\kappa_z}{\kappa_z+l_z}\right)\left[2\langle\varphi_{l_z}^+|\phi(\mathbf{Q},\omega,z)|\varphi_{l_z^0}^0\rangle+\frac{\kappa_z-l_z}{\sqrt{\kappa_z l_z}}\langle\varphi_{l_z}^-|\phi(\mathbf{Q},\omega,z)|\varphi_{l_z^0}^0\rangle\right], \tag{11}$$

where $\boldsymbol{\kappa}=(\mathbf{l}_\parallel^1,\kappa_z)$ is the momentum of the electron in vacuum and $\mathbf{Q}=\mathbf{l}_\parallel^1-\mathbf{l}_\parallel^0$.

Regarding the transport of the excited electrons to the surface, we follow the simple method used before [17,18,21], where the effect of inelastic collisions is included approximately through an exponential factor $e^{\mu z}$ which multiplies the electron final states inside the solid. The parameter $\mu$ is set to be proportional to $1/\lambda$, the inverse of the electron mean free path. Since the transport effects are expected to play only a minor role under the grazing scattering conditions, different choices of the parameter $\mu$ do not affect the calculation results appreciably. After inserting Eqs. (3) and (4) into Eq. (11), one obtains the full expression of the transition amplitude $\mathbf{M}_{\boldsymbol{\kappa}\leftarrow\mathbf{l}_0}=m_{\boldsymbol{\kappa}\leftarrow\mathbf{l}_0}\delta(\omega-\mathbf{Q}\cdot\mathbf{v}_\parallel)$, such that, for $z_0\geqslant 0$,

$$m_{\boldsymbol{\kappa}\leftarrow\mathbf{l}_0}=\frac{-i\tilde{\sigma}_n(Q)}{\pi Q}\left\{\frac{l_z^0}{l_z^0+ip}\left[I(p+i\kappa_z)+\frac{\kappa_z-l_z}{\kappa_z+l_z}I(p-i\kappa_z)\right]+\frac{\kappa_z}{\kappa_z+l_z}\frac{e^{-Qz_0}}{\epsilon_s(Q,\omega)+1}\left[J(\mu-i(l_z-l_z^0),0)+\frac{l_z^0-ip}{l_z^0+ip}J(\mu-i(l_z+l_z^0),0)\right]\right\}, \tag{12}$$

and, for $z_0<0$,

$$\begin{aligned}m_{\boldsymbol{\kappa}\leftarrow\mathbf{l}_0}=\frac{-i\tilde{\sigma}_n(Q)}{\pi Q}\Bigg\{&\frac{2\epsilon_s(Q,\omega,z_0)}{\epsilon_s(Q,\omega)+1}\frac{l_z^0}{l_z^0+ip}\left(\frac{1}{Q+p+i\kappa_z}+\frac{\kappa_z-l_z}{\kappa_z+l_z}\frac{1}{Q+p-i\kappa_z}\right)+\frac{\kappa_z}{\kappa_z+l_z}\Bigg[J(\mu-i(l_z-l_z^0),z_0)+\frac{l_z^0-ip}{l_z^0+ip}J(\mu-i(l_z+l_z^0),z_0)\Bigg]\\&-\frac{\kappa_z}{\kappa_z+l_z}\frac{\epsilon_s(Q,\omega,z_0)}{\epsilon_s(Q,\omega)+1}\Bigg[J(\mu-i(l_z-l_z^0),0)+\frac{l_z^0-ip}{l_z^0+ip}J(\mu-i(l_z+l_z^0),0)\Bigg]\Bigg\},\end{aligned} \tag{13}$$

where

$$I(a)=\left\{\frac{1}{Q+a}\left[\frac{\epsilon_s(Q,\omega)-1}{\epsilon_s(Q,\omega)+1}\right]-\frac{1}{Q-a}\right\}e^{-Qz_0}+\frac{2Qe^{-az_0}}{Q^2-a^2} \tag{14}$$

and

$$J(a,z_0)=\frac{2a}{Q^2-a^2}\left[\frac{2Q}{\pi}\int_0^\infty \frac{dk_z}{k_z^2+a^2}\frac{\cos k_z z_0}{\epsilon(k,\omega)}-\epsilon_s(Q,\omega,z_0)\right], \tag{15}$$

with $\omega=\mathbf{Q}\cdot\mathbf{v}_\parallel$.

We finally obtain the triple differential probability of the electron emission as a function of the position of the ion $z_0$ [22,24], viz.,

$$\frac{d^3P}{d\boldsymbol{\kappa}}=2\pi\int d\mathbf{l}_\parallel^0\rho_e\theta(E_F-\varepsilon_0)\,\theta(l_1^2-l_\parallel^2-\mathbf{Q}\cdot\mathbf{v}_\parallel)|m_{\boldsymbol{\kappa}\leftarrow l_0}|^2, \tag{16}$$

where $\rho_e=2$ takes account of the spin factor. The first step function confines the initial states of the electrons inside the Fermi sphere, while the second one assures that the emission constraint is met, $(l_z^0)^2=l_1^2-l_\parallel^2-\mathbf{Q}\cdot\mathbf{v}_\parallel\geqslant 0$. Since we are interested in the grazing scattering geometry, the total electron emission distribution will be obtained by integrating $d^3P/d\boldsymbol{\kappa}$ along the ion scattering trajectory, which will be discussed in the following section.

## III. SCATTERING TRAJECTORY

In the vicinity of surface, the motion of the incident ion is controlled by two kinds of forces. First, the ion is attracted by the dynamic image force and, as a result, its perpendicular velocity component $v_z$ increases. As the ion approaches the first atomic plane, the repulsive forces due to the continuum planar potential grow stronger causing specular reflection of the ion. From Eqs. (3) and (4), the induced potential can be written as

$$\phi_{ind}(\mathbf{r},t)=\frac{1}{2\pi}\int\frac{d\mathbf{Q}}{Q}\tilde{\sigma}_n(Q)F(Q,\omega,z,z_0)e^{-i\mathbf{Q}\cdot(\mathbf{R}-\mathbf{v}_\parallel t)}, \tag{17}$$

where the function $F(Q,\omega,z,z_0)$ is given, for the ion moving in the vacuum ($z_0>0$ and $z>0$) by

$$F(Q,\omega,z,z_0)=\frac{\epsilon_s(Q,\omega)-1}{\epsilon_s(Q,\omega)+1}e^{-Q(z+z_0)},$$

and, for the ion inside the target ($z_0<0$ and $z<0$), by

$$F(Q,\omega,z,z_0)=\epsilon_s(Q,\omega,z-z_0)+\epsilon_s(Q,\omega,z+z_0)-\frac{2\epsilon_s(Q,\omega,z_0)\epsilon_s(Q,\omega,z)}{1+\epsilon_s(Q,\omega)}-e^{-Q|z-z_0|}.$$

The surface image potential, i.e., the classical self-energy of the ion, can be expressed as $U_s(z_0)=(1/2)\int d\mathbf{r}\rho_{ext}(\mathbf{r},t)\phi_{ind}(\mathbf{r},t)$, which, with Eq. (17), gives

$$U_s(z_0)=\frac{1}{4\pi}\int\frac{d\mathbf{Q}}{Q}[\tilde{\sigma}_n(Q)]^2F(Q,\omega,z_0,z_0). \tag{18}$$

On the other hand, the surface continuum planar potential $U_p(z)$ can be easily obtained from the Molière's approximation [33]. So, in the laboratory frame of reference, the equation of motion in the direction perpendicular to the surface can be written as

$$m\frac{dv_z}{dt}=-\frac{\partial U_p(z_0)}{\partial z_0}-\frac{\partial U_s(z_0)}{\partial z_0}, \tag{19}$$

where $m$ is the ion mass. Denoting the initial kinetic energy of the incident ion by $E=(1/2)mv^2$, and using $mdv_z/dt=d(mv^2/2)/dz_0$, we can integrate Eq. (19) over $z_0$ to obtain the equation for the trajectory of the ion undergoing specular reflection at the glancing angle $\alpha$,

$$\frac{dx}{dz_0}=\mp\frac{1}{\alpha\sqrt{1-\dfrac{U_p(z_0)+U_s(z_0)}{E\alpha^2}}}, \tag{20}$$

where $\mp$ correspond to the incoming and outgoing parts of trajectory, respectively. Note that the position of closest approach to the surface $z_m$ is given by $E\alpha^2=U_p(z_m)+U_s(z_m)$.

Since the motion perpendicular to the surface proceeds adiabatically on the time scales relevant for electron excitation processes, the total electron emission probability can be obtained by integration of Eq. (16) along the ion trajectory,

$$\frac{d^3P}{d\vec{\boldsymbol{\kappa}}}=4\pi\int_{z_m}^\infty dz_0\frac{dx}{v\,dz_0}\int d\mathbf{l}_\parallel^0\rho_e\theta(E_F-\varepsilon_0)\times\theta(l_1^2-l_\parallel^2-\mathbf{Q}\cdot\mathbf{v}_\parallel)|m_{\boldsymbol{\kappa}\leftarrow\mathbf{l}_0}|^2. \tag{21}$$

Note that the scattering trajectory is generally not symmetrical about the turning point $z_m$ due to the effects of the projectile charge-state evolution in the course of scattering. However, we neglect these effects and assume the trajectory to be symmetrical, which is reasonable approximation, given that the incident and scattered angles are of the order of milliradians and that the ions enter the target up to the depths which are not larger than the average atomic radius.

Before Eq. (21) could be used, one has to specify the models for the dielectric function $\epsilon(k,\omega)$ and for the ionization degree $q(z_0)$. As was done before [26], we use two different forms of the dielectric function, the local-field-corrected one and the plasmon-pole approximation, for the cases of low and high ion velocities, respectively. These choices have been shown to be both suitable and appropriate in the work on energy losses [26], making it easy to analyze the contributions from both the collective and the single-electron excitations. On the other hand, the evolution of the ionization degree in grazing scattering is not well understood at present. When the projectile approaches the surface, it experiences electron-capture and -loss processes due to collisions with the surface atoms. Slow ions are largely neutralized by electron transfer before they reach the distance of closest approach. At high velocities, however, the ions may enter the electron gas deeper during a shorter interaction time, and be exposed to the electron loss as well as electron

capture processes. Thus, the charge exchange in the vicinity of the topmost atomic layer will be so intense that the charge state will become equilibrated within a short path length. We adopt the model developed in the previous work, where a double exponent and a linear interpolation, combined with a velocity-dependent electron-stripping model, were used to describe the position-dependent charge states of slow and fast incident ions, respectively [26].

## IV. RESULTS OF THE CALCULATION

In this work, we study grazing scattering of ions from an aluminum surface, characterized by the Fermi velocity $v_F = 0.92$ a.u., the work function $\Phi = 0.156$ a.u., and the damping coefficient in the dielectric function $\gamma = 0.037$ a.u. In Fig. 1, we show the differential probability $d^3P/d\boldsymbol{\kappa}$ as a function of the electron energy for $C^{3+}$ ions incident on an Al surface with different incident angles $\alpha$ and with the speed $v = 3$ a.u. Figures 1(a)–1(c) correspond to three different observation angles $\beta$ with respect to the surface plane. Under these conditions, the electrons in the electron gas above the topmost atomic layer are excited by the decay of the surface plasmon and are emitted from the surface, producing the energy spectrum with a broad maximum at around $\omega_s - \Phi = 6.9$ eV, which is seen in Fig. 1. It is also seen that such a structure of the emitted spectra is largely independent of the emission angles and the incident angles. The peak widths are the consequences of the surface-plasmon dispersion within the specular-reflection model. There are no signatures of the bulk-plasmon excitation and decay in Fig. 1, because the incident ions have been scattered away by the atoms in the first layer before they could penetrate into the solid. One can also see in Fig. 1 that, as the incident angles increase, the peak values of the emission spectra also increase, which should be attributed to the increasing depth of penetration of ions in the electron gas and, consequently, longer time spent in interactions with electrons. Considering the dependence on the emission angle $\beta$ in Fig. 1, we find that the peak values pass through a broad maximum at around $\beta = \pi/3$, which is similar to the conclusion drawn by other authors [18].

Figure 2 shows the electron emission at several observation angles $\beta$ for $N^+$ ions scattered from an Al surface with relatively low velocity of $v = 0.5$ a.u. under different angles of incidence. The electron spectra exhibit peaks at low energies, and the maximum values of the electron emission are seen to increase with increasing angles of incidence, in a way similar to Fig. 1. These peaks occur at the emission energies which increase from about 1 eV to about 5 eV as the observation angles decrease, which is in contrast to the stability of the peak positions for fast ions, seen in Fig. 1. Such a behavior of the peak energies may be explained, based on the expression $\omega = \mathbf{Q} \cdot \mathbf{v}_{\parallel}$, as being due to the momentum transfer in the direction of the ion motion. This is also corroborated by the fact that the peak values of electron emission increase as the observation angle decreases, that is, as the observed emission occurs closer to the direction of motion of the projectile.

It has been shown that the threshold velocity for excitation of a bulk-plasmon resonance via direct interaction with the ion is $v_{th} \approx 1.3 v_F$, based on the constraints due to the momentum and energy conservation [15]. However, recent experiments have found structures in the emitted electron spectra induced by slow ions on solid surface, which display low-energy maxima, reminiscent of the plasmon resonance [9,13]. Some of these low-energy projectiles were incident at grazing angles and were not expected to penetrate into the

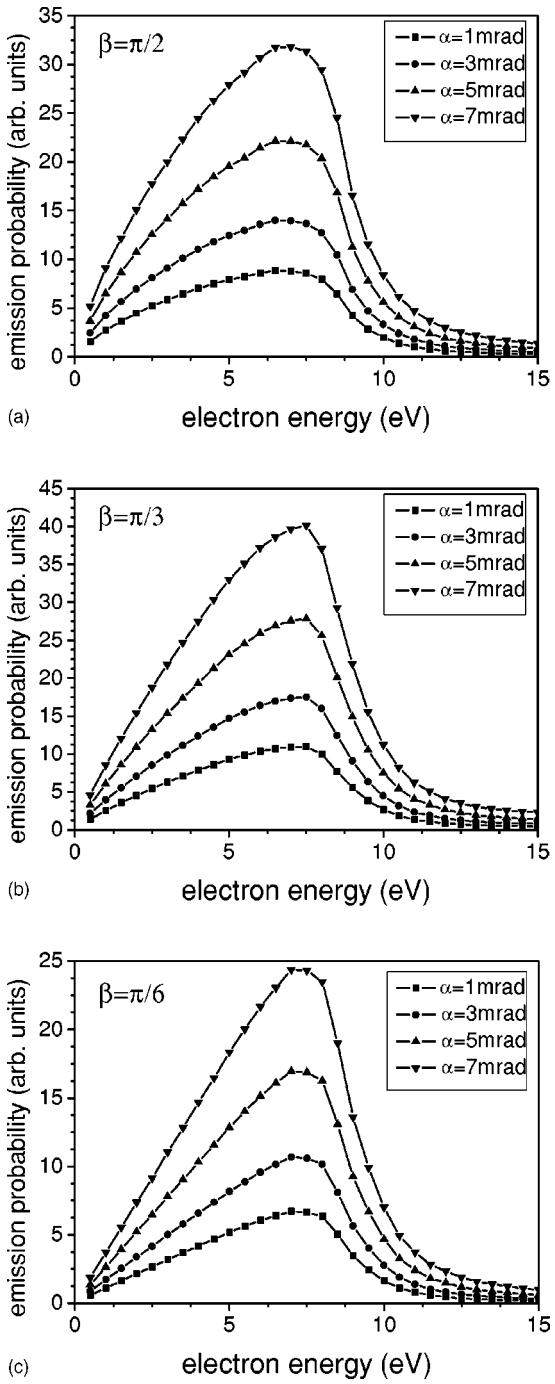


FIG. 1. Differential probability of electron emission vs the electron energy, induced by $C^{3+}$ ions incident on an Al surface with the velocity of $v = 3$ a.u. at various glancing angles of incidence $\alpha$. Results are shown for three electron emission angles relative to the surface: (a) $\beta = \pi/2$, (b) $\beta = \pi/3$, and (c) $\beta = \pi/6$.

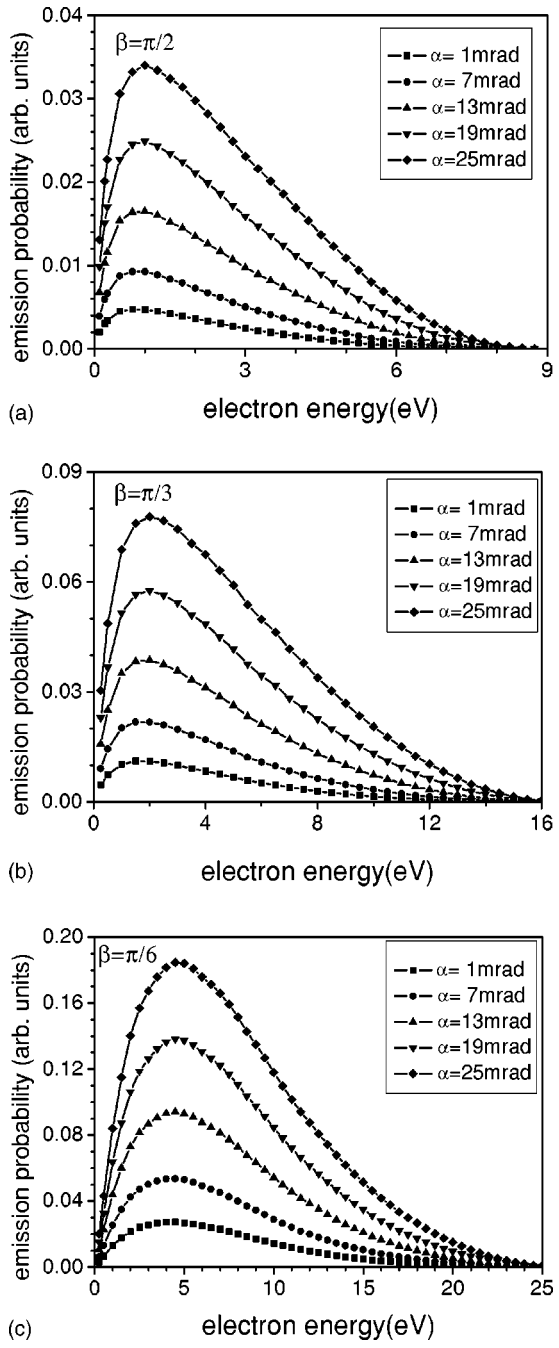


FIG. 2. Differential probability of electron emission vs the electron energy, induced by $N^+$ ions incident on an Al surface with the velocity of $v=0.5$ a.u. at various glancing angles of incidence $\alpha$. Results are shown for three electron emission angles relative to the surface: (a) $\beta=\pi/2$, (b) $\beta=\pi/3$, and (c) $\beta=\pi/6$.

solid. Several mechanisms were discussed to explain the plasmon excitation by ions moving at velocities much lower than $v_{th}$, such as Auger capture process, Auger decay of inner-shell vacancies, shake-up during the capture of an electron, or secondary collisions with high-energy electrons [12]. However, none of these mechanisms has been included in our theoretical model of KEE, so that the lack of signature of plasmon decay in the electron spectra in Fig. 2 suggests that the electron emission induced by slow ions is mainly due to the single-electron excitation mechanism in the present model.

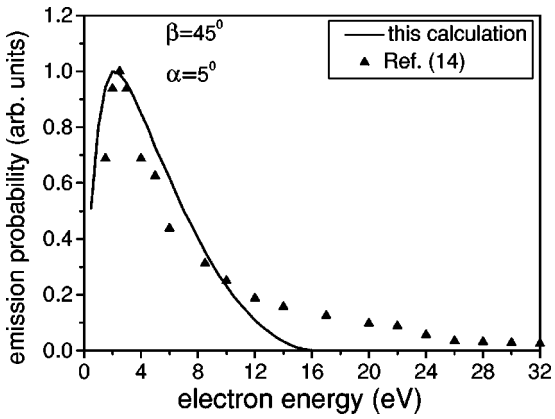


FIG. 3. Differential probability of electron emission vs the electron energy, induced by 5-keV $H^+$ ions incident on an Al surface under angle $\alpha=5°$, with the electron emission angle $\beta=45°$. Results of our calculation (solid line) are compared with the experimental data from Ref. [14] (solid triangles).

For the sake of comparison, we show in Fig. 3 the experimental data from Ref. [14] for electron emission after grazing scattering of 5-keV $H^+$ ions from Al(111) surface with the incident angle $\alpha=5°$ and the emission angle $\beta=45°$ along with the result of our calculations with these parameters. The agreement of our model with the experiment is fairly good up to around the electron energy of $\omega_p-\Phi \approx 11$ eV, which corresponds to the bulk-plasmon resonance. While the precise mechanism of plasmon excitation under such conditions is yet to be identified [14,15], the broad tail in the experimental data in Fig. 3, above the energy 11 eV, can be ascribed to the electron emission due to plasmon decay into electron-hole pairs. On the other hand, the agreement our model with the experiment at energies below 11 eV indicates that the main contribution to electron emission for these energies comes from the single-electron excitation mechanism.

The dependences of the electron emission spectra on the initial charge states of the incident ions are shown in Figs. 4 and 5, indicating that, as the ion charge increases, more electrons are excited and emitted, for both high (Fig. 4) and low (Fig. 5) ion velocities. This significant feature of the increase of the electron yield with increasing charge state has also been observed experimentally for $Ne^{q+}$ ion impact on an Al surface [10], where it was explained by the onset of potential electron emission (PEE). Considering that the PEE is roughly proportional to the potential energy of the incident ion, it is clear that the multiply charged ions will induce a strong PEE. Since our model for KEE does not include any charge transfer of the Auger type capable of inducing PEE, it is remarkable that the results in Figs. 4 and 5 show that KEE may be so strongly influenced by different ion charge states, prior to the neutralization (for slow ions) or charge equilibration (for fast ions) at the solid surface. This shows that the charge-state-dependent induced potential exerts a strong influence on the electron excitation mechanisms in KEE, even when the ion is at large distances from the surface.

The effects of the ion velocity on the electron emission

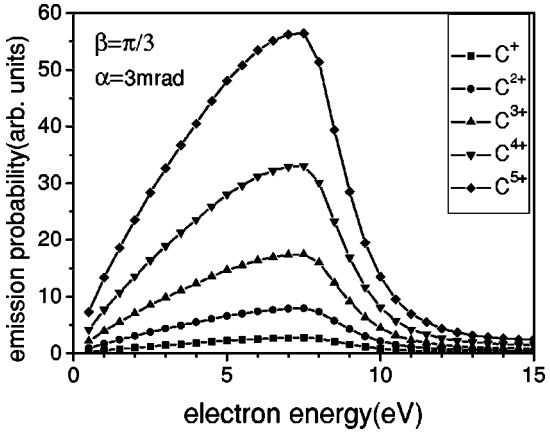


FIG. 4. Differential probability of electron emission vs the electron energy, induced by $C^{q+}$ ions with various charge states $q$, incident on an Al surface with the velocity of $v=3$ a.u. at the glancing angle of incidence $\alpha=3$ mrad. The electron emission angle relative to the surface is $\beta=\pi/3$.

are shown in Figs. 6 and 7. For low velocities, in Fig. 7, the emission peak grows higher and wider with increasing projectile velocity, similar to the experimental data in Refs. [9,12]. However, for high velocities in Fig. 6, the peak values of the electron emission grow through a maximum at a medium velocity and continue to decrease as the ion velocity continues to increase. This roughly corresponds to the well-known dependence of the ion energy loss on its velocity. On the other hand, the peak position in Fig. 6 occurs at around 6.9 eV, the value characteristic for the plasmon decay, when the velocity is high, but keeps increasing as the ion velocity decreases down to the medium range. This probably indicates a strong mixing of the plasmon decay and the single-electron excitation mechanisms for intermediate ion velocities, where the momentum transfer to the emitted electron may become more prominent.

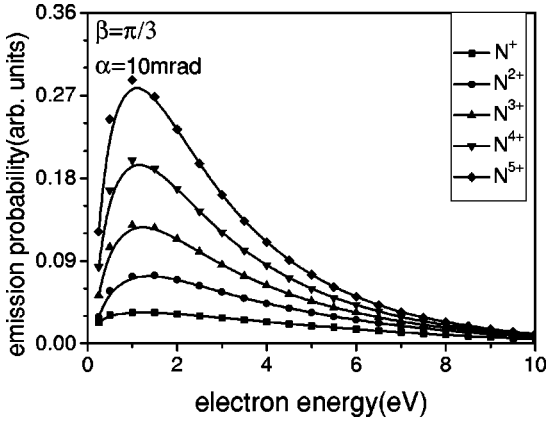


FIG. 5. Differential probability of electron emission vs the electron energy, induced by $N^{q+}$ ions with various charge states $q$, incident on an Al surface with the velocity of $v=0.5$ a.u. at the glancing angle of incidence $\alpha=10$ mrad. The electron emission angle relative to the surface is $\beta=\pi/3$.

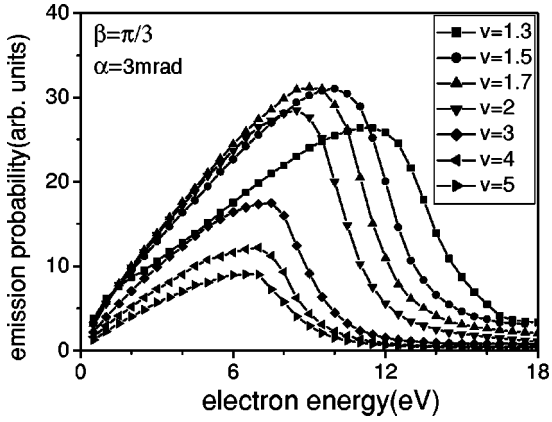


FIG. 6. Differential probability of electron emission vs the electron energy, induced by $C^{3+}$ ions incident on an Al surface with several velocities $v$ at the glancing angle of incidence $\alpha=3$ mrad. The electron emission angle relative to the surface is $\beta=\pi/3$.

## V. SUMMARY

We have developed a theoretical model for calculation of the kinetic electron emission (KEE) differential probabilities for grazing scattering of heavy ions from a surface, at high or low incident velocities. The energy spectra of emitted electrons have been obtained on the basis of the first-order, time-dependent perturbation theory with the electron states calculated from Schrödinger equation with a finite-step-barrier potential. The response of the surface has been expressed by means of the dielectric theory with the specular reflection model, whereas the local-field correction and the plasmon-pole approximation were used for slow and fast ions, respectively. The distributions of the electrons bound to the incident ion have been taken into account by using the BK model, where a double-exponent model and a linear interpolation model were employed to describe the position-dependent ionization degree throughout the scattering process, for slow and fast projectiles, respectively.

The dependences of the differential probability on the electron energy and the emission angle have been discussed

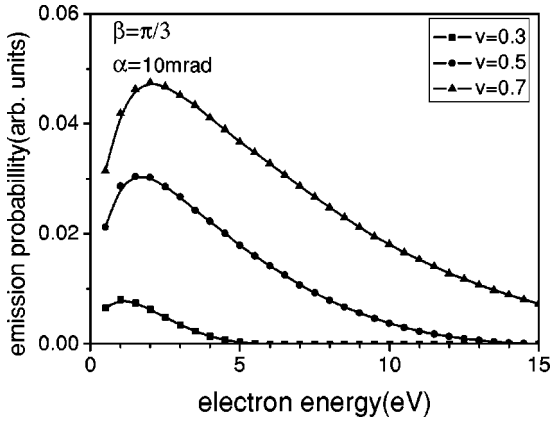


FIG. 7. Differential probability of electron emission vs the electron energy, induced by $N^{+}$ ions incident on an Al surface with several velocities $v$ at the glancing angle of incidence $\alpha=10$ mrad. The electron emission angle relative to the surface is $\beta=\pi/3$.

for different incident ion velocities, angles, and charge states. Most of our results show the electron spectra similar to those obtained in various experiments or theoretical accounts [8–12,16–18]. As expected, the electron emission induced by grazing scattering of fast ions at surfaces shows a peak in the energy spectra at the position given by the surface-plasma frequency minus the work function, as a result of the surface-plasmon excitation and its subsequent decay. For slow ions, the peaks in the energy spectra are located somewhere from 1 eV to 4 eV, depending on the observation angle, and are ascribed to the single-electron excitation mechanism. The absence of the signature of the plasmon decay in the emitted spectra for slow ions is a consequence of the fact that the plasmon excitation mechanism does not operate in our model of KEE when the ion velocities are below the kinematic threshold value. Of course, other mechanisms, beyond the scope of our work, may be responsible for the experimentally observed characteristic features in the electron emission spectra induced by slow ions, which warrants further efforts to amend the present model. Finally, strong effects of the initial ion charge states have been shown in our calculations of the electron spectra, indicating that a further study is recommended regarding the role of the projectile charge states in KEE induced by grazing scattering of heavy ions.

## ACKNOWLEDGMENTS

This work was jointly supported by the National Natural Science Foundation of China (Grant No. 10275009, Y.N.W.) and the Grant for Striding-Century Excellent Scholar of the Ministry of Education, State of China. Z.L.M. acknowledges the support by the Natural Sciences and Engineering Research Council of Canada.

[1] R.J. MacDonald, D.J. O'Connor, J. Wilson, and Y.G. Shen, Nucl. Instrum. Methods Phys. Res. B **33**, 446 (1988).
[2] M.H. Shapiro and T.A. Tombrello, Nucl. Instrum. Methods Phys. Res. B **90**, 473 (1994).
[3] S.J. Timoner, M.H. Shapiro, and T.A. Tombrello, Nucl. Instrum. Methods Phys. Res. B **114**, 20 (1996).
[4] A. Arnau *et al.*, Surf. Sci. Rep. **27**, 113 (1997).
[5] C. Benazeth, N. Benazeth, and L. Viel, Surf. Sci. **78**, 625 (1978).
[6] D. Hasselkamp and A. Scharmann, Surf. Sci. **119**, L388 (1982).
[7] N.J. Zheng and C. Rau, J. Vac. Sci. Technol. A **11**, 2095 (1993).
[8] A. Hegmann, R. Zimny, H.W. Ortjohann, H. Winter, and Z.L. Mišković, Europhys. Lett. **26**, 383 (1994).
[9] R.A. Baragiola and C.A. Dukes, Phys. Rev. Lett. **76**, 2547 (1996).
[10] D. Niemann, M. Grether, M. Rösler, and N. Stolterfoht, Phys. Rev. Lett. **80**, 3328 (1998).
[11] S.M. Ritzau, R.A. Baragiola, and R.C. Monreal, Phys. Rev. B **59**, 15 506 (1999).
[12] E.A. Sánchez, J.E. Gayone, M.L. Martiarena, O. Grizzi, and R.A. Baragiola, Phys. Rev. B **61**, 14 209 (2000).
[13] N. Stolterfoht, D. Niemann, V. Hoffmann, M. Rösler, and R.A. Baragiola, Phys. Rev. A **61**, 052902 (2000).
[14] H. Winter, H. Eder, F. Aumayr, J. Lörincik, and Z. Sroubek, Nucl. Instrum. Methods Phys. Res. B **182**, 15 (2001).
[15] R.A. Baragiola, C.A. Dukes, and P. Riccardi, Nucl. Instrum. Methods Phys. Res. B **182**, 73 (2001).
[16] D.L. Mills, Surf. Sci. **294**, 161 (1993).
[17] F.J. García de Abajo and P.M. Echenique, Nucl. Instrum. Methods Phys. Res. B **79**, 15 (1993).
[18] F.J. García de Abajo, Nucl. Instrum. Methods Phys. Res. B **98**, 445 (1995).
[19] R.H. Ritchie and A.L. Marusak, Surf. Sci. **4**, 234 (1966).
[20] D. Wagner and Z. Naturforsch, Z. Naturforsch. Teil A **21**, 634 (1966).
[21] M.L. Martiarena, E.A. Sánchez, O. Grizzi, and V.H. Ponce, Phys. Rev. A **53**, 895 (1996).
[22] M.S. Gravielle, Phys. Rev. A **58**, 4622 (1998).
[23] M.S. Gravielle, Phys. Rev. A **62**, 062903 (2000).
[24] M.S. Gravielle and J.E. Miraglia, Phys. Rev. A **65**, 022901 (2002).
[25] A. Niehaus, P.A. Zeijlmans van Emmichoven, I.F. Urazgil'din, and B. van Someren, Nucl. Instrum. Methods Phys. Res. B **182**, 1 (2001).
[26] Y.H. Song, Y.N. Wang, and Z.L. Mišković, Phys. Rev. A **63**, 052902 (2001).
[27] J.I. Juaristi, A. Arnau, P.M. Echenique, C. Auth, and H. Winter, Phys. Rev. Lett. **82**, 1048 (1999).
[28] M. Fritz, K. Kimura, H. Kuroda, and M. Mannami, Phys. Rev. A **54**, 3139 (1996).
[29] W. Brandt and M. Kitagawa, Phys. Rev. B **25**, 5631 (1982).
[30] P.M. Echenique, F.J. García de Abajo, V.H. Ponce, and M.E. Uranga, Nucl. Instrum. Methods Phys. Res. B **96**, 583 (1995).
[31] H. Bethe and Edwin Salpeter, *Quantum Mechanics of One and Two-Electron Atoms* (Springer-Verlag, Berlin, 1957).
[32] R.E. Wilems, Ph.D. thesis, University of Tennessee, 1968 (unpublished).
[33] Y.H. Ohtsuki, *Charged Beam Interaction with Solids* (Taylor & Francis, London, 1983).